

Response to Reviewers

Manuscript: ACP-2017-842

Manuscript title: Investigating biomass burning aerosol morphology using a laser imaging nephelometer

The discussion below includes the complete text from the reviewer (bold), along with our responses to the specific comments and the corresponding changes (additions in italics, deletions struck through) made to the revised manuscript. All line numbers refer to the original manuscript.

Response to Reviewer #1 Comments:

This paper presents very interesting data on the scattering phase function of aerosol emitted from biomass burning. There is a strong need for a better quantification of the scattering properties of non-spherical particles. I, therefore, fully agree with the authors' sentence on page 12 that "It would be useful to collect more information about how the morphology of fresh emissions evolves with aging in the atmosphere". The data obtained here are very encouraging regarding the ability of this new instrument to provide this kind of data that can aid radiative forcing calculations as well as remote sensing retrievals. I, therefore, strongly support the publication of this paper.

General comments:

The paper is very well written and the experiments have been mostly well described, and for the most part, well justified. I think the paper can be published almost as is, with just a few minor clarifications and additions that I will discuss next.

We are grateful for the reviewer's very positive comments, and appreciate that they took the time to review the manuscript carefully. We have tried to address their suggestions and concerns to the best of our ability individually below.

Specific comments:

- Introduction

* Page 2, lines 19-29: An interesting recent approach for determining the shape of coarse particles is provided by Berg et al., Solving the inverse problem for coarse-mode aerosol particle morphology with digital holography. *Scientific reports*, 2017. 7(1): p. 9400.

We thank the reviewer for bringing our attention to this paper, which indeed shows a very sophisticated method to measure morphology of coarse mode particles in an uninterrupted aerosol flow. We have added the following to the appropriate paragraph:

P.2 L.29: “Recently, a sophisticated method for determining the morphology of coarse mode aerosol using holographic imaging without interrupting the aerosol flow was demonstrated (Berg et al., 2017), however this method is unfeasible for accumulation mode particles.”

* Page 2 bottom, and 3 top. There are also commercial nephelometers that measure the backscattering at different angles by adjusting the backscattering arm angle. Maybe this could be mentioned here. See, for example, Chamberlain-Ward et al., Advances in Nephelometry through the Ecotech Aurora Nephelometer” The Scientific World Journal, vol. 11, Article ID 310769, 6 pages, 2011.

The reviewer is right to point out that we did not mention nephelometers that allow the user to set the backscatter angular coverage. We have adjusted the text (added text in italics, removed text struck through) as follows:

P.3 L.1-3: "...integrating nephelometers (Anderson et al., 1996). *Some nephelometers also have an option to measure set angular regions by blocking portions of the forward scattered light (Chamberlain-Ward and Sharp, 2011).* While these devices are reliable and robust, the hemispheric measurements over large portions of the phase function do not provide much information about particle morphology due to the lack of angular specificity."

- Experimental

* At the beginning of the section: It would be nice to mention the reasons for the choice of the specific wavelengths. Why these and why so close to each other?

The two wavelengths were chosen with the hope of seeing more evidence of absorption by brown carbon particles in the phase functions measured at 375 nm compared to those measured at 405 nm. Unfortunately, as absorption predominantly affects the backscatter, where the signal is relatively low, we were unable to observe wavelength-dependent differences under these experimental conditions. In the future, we may try to do so by increasing the laser power (which would saturate the CCD at forward scatter angles) to have better signal-to-noise in the backscatter region. To address the question, we have added the following to the first paragraph of the Experimental section:

P.4 L.6: "...120 mW respectively. *These wavelengths were selected under the hypothesis that increased absorption by brown carbon particles at 375 nm compared 405 nm may be observable in the measured phase functions, however we were unable to observe this under the experimental conditions.* The output beams..."

* Why is the polarization converted to circular? It would be useful to explain the reason. Could one switch the polarization periodically from vertical to horizontal to collect images at different polarizations and possibly gain further insights on the shape of the particles? If not why? Or just a practical choice?

The use of circularly polarized light is, essentially, a practical decision since it eliminates the need to switch polarization (effectively halving the acquisition rate). In the future, we may adjust the instrument to have this capability since the depolarization ratio provides additional information, particularly for larger (especially dust) particles. We have altered the text as follows:

P.4 L.8: "...sample chamber. *The circular polarization of the beam allows retrieval of the unpolarized phase function, for a homogeneous sample (Bohren and Huffman, 1983), simplifies the experimental set-up by eliminating the need for a variable waveplate (Dolgos and Martins, 2014), and maximizes the data acquisition rate by only recording the phase function under one polarization condition at each wavelength.* A set of apertures..."

* Also, it would be good to provide some details about the beam quality, the noise and the stability of the lasers and provide some information on the set of apertures.

The reviewer raises a few valid points here, which we will address one-by-one.

We can infer the beam quality by looking at images of phase functions due solely to Rayleigh scattering. Since the number density of gas molecules will be homogeneous throughout the beam volume, we

assume that variations in pixel intensity over a single angle bin are due solely to the intensity profile of the laser beam. To demonstrate that the beam profile is Gaussian, we added an additional figure to the Supplementary (shown below), and added a brief reference to it in the main text. Note that the figure labels in the Supplementary have been changed to follow the order of the main manuscript.

P.4 L.9-10: “The two beams traveled the same beam path inside the chamber, with collimated diameters of approximately 3 mm, *and exhibited Gaussian intensity profiles (see Figure S1).*”

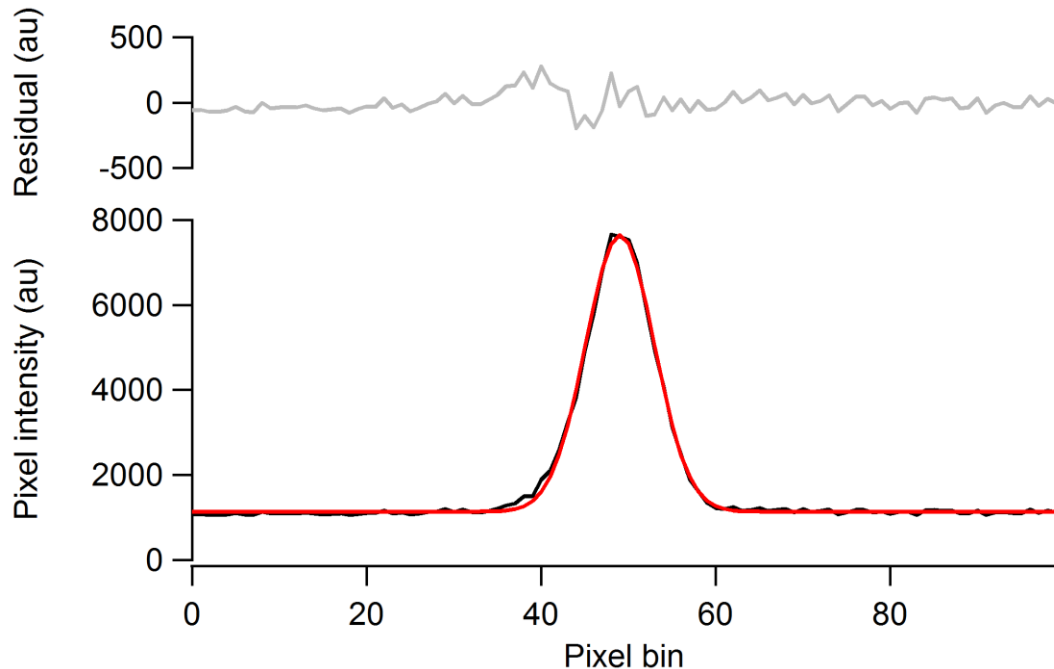


Figure S1: Measured pixel intensity across the 14° scattering angle bin (black) is shown compared with Gaussian fit (red) for a single CCD image (1 sec integration time) when the imaging nephelometer is filled with filtered air and signal arises solely from Rayleigh scattering. The residual (grey) demonstrates the quality of the fit.

With regards to the laser power stability, we account for any significant (≥ 1 mW) drifts in laser power by reading the power at the diode head for each individual image acquisition (and then apply a calibration factor to convert diode head power to the actual power that reaches the sample chamber). More minor power drifts, if important for the retrieved information, would likely appear as a turning point in the Allan-Werle deviation plots in the Supplementary, which we do not observe over timescales of ~ 1 hour. Short-term fluctuations in power may contribute to noise in the total integrated scattering retrieved for the imaging nephelometer (which is, however, less significant than the noise of the integrating nephelometer measurements), however these are largely removed for the phase functions presented by averaging multiple images.

More details were added about the apertures:

P.4 L.8-9: “A set of *three* apertures (4 mm diameter) blocked stray light before the beam passed through the aerosol sample.”

* On page 5 at the top: The Rayleigh scattering contribution is calculated based on pressure and temperature. What composition is assumed here? Is there any potential for biases due to gases specific to air in which the aerosol are transported? For example, NO₂ (although that was probably

removed by the scrubber)? In other words, was there any attempt to compare this with measurements of just aerosol-free air using a filter.

We have clarified the Rayleigh scattering calculation (see below) in the manuscript. In general, the sample aerosol and dilution air were denuded (including of NO₂) and dried, and therefore no corrections were applied to the literature value for Rayleigh scattering of clean dry air. We have added a comment on the maximum possible effect of CO₂ (modern-day compared to 1950s standard air) on the Rayleigh scattering cross-section, which was extremely small (0.03%). In the laboratory, we did also measure the Rayleigh scattering of pure CO₂ and obtained the same calibration curve, within the noise of the measurements, when using Rayleigh scattering cross-sections from the literature (same source as identified below).

P.4 L.31-32: “This correction factor was determined daily using Rayleigh scattering from dried and filtered ambient air, *and Rayleigh scattering coefficients for dry air from the literature (Bodhaine, 1979; Penndorf, 1957). Since the air was dried and scrubbed, corrections for additional water vapor or NO₂ were not needed; likewise, corrections for higher modern-day levels of CO₂ were deemed unnecessary since additional CO₂ (compared to “standard air” in the 1950s (Penndorf, 1957)) would result in a maximum error of 0.03% in the Rayleigh scattering cross-section.* The consistency of the calibration...”

*** On page 6, line 27: 5 nm coating is quite thick when compared with ~50 nm soot monomers (see below on the monomer diameter, as well). That might also affect how coated the particles might appear vs be “naturally”.**

We used the minimum recommended coating thickness to prevent charging of samples under the electron beam. While it is true that this might make soot particles appear to be less clearly composed of individual monomers, it should not be sufficient to cause freshly emitted soot (i.e. mostly un-collapsed) from appearing very “branchy” (i.e. having low D_f values). We did take into account the coating when retrieving the monomer size from SEM images. While it was difficult to distinguish different monomers, we could measure the narrowest width of fractal branches for a variety of particles (which generally were between 60 – 65 nm in the raw image). Therefore, we hypothesized that 50 nm was likely representative of the monomer diameter, and this agreed well with the literature. However, we have adjusted the text slightly to account for the uncertainty associated with sputter coating thickness (5 nm is the maximum thickness based on the sputter coating duration):

P. 6 L.27: “...later sputter coated with *up to* 5 nm of platinum...”

*** Page 7, line 10: the fractal-like structure depends also on the presence of co-emitted components that might condense on the soot and restructure it.**

This is a good point. We have added a justification for why we assumed no significant collapse of black carbon fractals (due to the low relative humidity conditions).

P.7 L.10-11: “Since fresh (< 4 hrs) emissions were measured in the absence of sunlight, it is unlikely that significant oxidative aging occurred in the smoke chamber. *The smoke chamber relative humidity was less than 40% for all fires measured, so we assume there was no significant restructuring of the black carbon agglomerates by organic or sulfuric acids (Xue et al., 2009; Zhang et al., 2008).*”

*** Page 7, line 16: It might be good to cite Sorensen’s review paper here as well (it is cited a few sentences later on, but it seems to fit here too).**

We have added the citation to Sorensen 2001 (alongside the Chakrabarty and Liu citations, P.7 L.16).

* Page 8, lines 14-17: Some more details here would be useful. How did you get the total scattering from the LAS? How was the match performed? What algorithm was used? etc.

We have added the following section of text to the Supplementary (as well as a reference to it in the main manuscript) to hopefully clarify how the LAS measurements were utilized, specifically with regards to fractal particles:

"The LAS retrieves aerosol size distributions based on scattered 633 nm light. According to the manufacturer's specifications, the light collecting optics cover the solid angles $90^\circ \pm 57^\circ$, excluding $90^\circ \pm 14.8^\circ$. This translates to $33^\circ - 75.2^\circ$ and $104.8^\circ - 147^\circ$ of the scattering phase function with a maximum azimuthal (out of the plane of the phase function) angle of 57° at 90° scattering angle. This means that, for any given phase function, we can calculate the fraction of scattered light theoretically collected and measured by the LAS detection system. Multiplying this fraction by the integrated scatter in absolute units gives the total scatter measured by the LAS. Since the LAS is calibrated for nominally spherical ammonium sulfate particles, we use Mie theory to determine the total scattered measured per particle for each size bin (99 bins). Then, using the parameterizations of k_o , D_f , and a described in Section 3.1, we adjust the magnitude of N_p (the number of monomers per agglomerate) to match the scatter measured by the LAS for each size bin (based on RDG calculations). Thus, we can approximately correlate LAS size bins with fractal sizes."

* Page 8, line 17: Monomers diameter might change quite a bit depending on the specific combustion conditions (for example, even for the specific of biomass burning, in the paper by China et al. (2003) cited earlier on in the manuscript, the monomers had diameters from 37 to 56 nm). Did the author estimate the diameter from their SEM images? Would the exact diameter value make a large difference in the comparison when using RDG? Similar comments apply to the effect of K0 and Df. Although some of these aspects are touched upon later in the paper.

As mentioned in the manuscript, we did estimate the spherule size from SEM micrographs (taking into account the added Pt coating thickness). While the RDG phase functions are sensitive to D_f , k_o , and a , we chose not to comprehensively cover the full range of possible values for the RDG parameterization since the aim of the paper is mainly to serve as a demonstration of the instrumental capabilities. We have added a section to the text to try to convey this more clearly:

P.8 L.19-20: "As mentioned, the values of D_f and k_o were taken to be 1.85 and 2.77, respectively, based on reported fractal-like aerosol measurements in the literature, particularly for biomass burning emissions. While the phase functions modeled using RDG are sensitive to these values, as well as the monomer diameter, a comprehensive analysis of the full range of possible RDG parameterization is beyond the scope of this paper; rather, here we present an initial "best guess" of the RDG parameterization based on the limited literature on biomass burning-produced soot and SEM micrographs. Spherical particles were assumed to be predominantly organic material..."

- Results and discussion

* At the beginning of the section, while discussing the performance of the instrument: It might be useful, for the purpose of comparing the performance of this instrument to the other more widely used techniques, to also calculate Allan-Werle variances for the TSI and the CRD-PAS instruments.

To better convey the relative performance of the three scattering measurements, we have included the following text and figure in the Supplementary:

“Figure S2-S4 shows an Allan-Werle deviation plot for scattering signal integrated over a single angle bin (each $\sim 0.5^\circ$) at several measurement angles. This was determined by continuously imaging the phase function of a clean air sample and removing the Raleigh scattering component to measure a “zero” phase function. Figure S5 shows the Allan-Werle deviation plot for the total integrated scatter at 405 nm for the TSI integrating nephelometer (red) and laser imaging nephelometer (black). Note that the integrating nephelometer has an acquisition rate of 1 Hz for each channel, while the imaging nephelometer has an average acquisition rate of 0.2 Hz. The integrating nephelometer scattering was scaled from 450 nm (observed) to 405 nm using the measured scattering Ångstrom exponent between 450 and 550 nm. The normal mode of operation for the CRD PAS during these experiments included automatic re-zeroing every six minutes, therefore these data are not included in the Allan-Werle plot; the accuracy of both the absorption and extinction channels is $\pm 5\%$. Details of the CRD PAS can be found in Lack et al. (2012).”

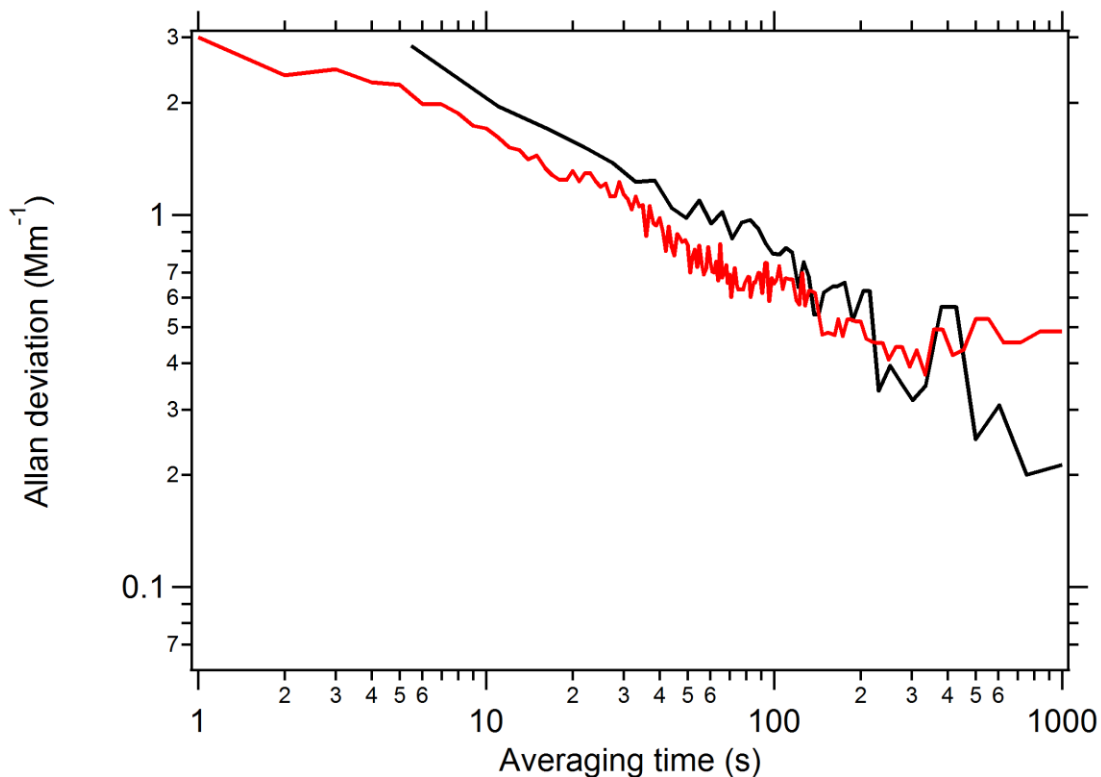


Figure S5: Allan-Werle deviation plot of integrated scatter at 405 nm for the imaging nephelometer (black) and integrating nephelometer (red). The integrating nephelometer measurements at 450 nm were scaled to 405 nm using the measured scattering Ångstrom exponent between 450 and 550 nm. Instruments were co-sampling filtered air.

* Page 9, line 24: a work that might be worth mentioning here is also that by Liu et al., Aerosol single scattering albedo dependence on biomass combustion efficiency: Laboratory and field studies. Geophysical Research Letters, 2014. 41(2): p.2013GL058392.

We thank the reviewer for the suggestion, the Liu et al. citation and a reference to Pokhrel et al. 2016 have been added (along with Selimovic et al. 2017, P.9 L.24).

* Page 10, lines 17-19: Is there any guess on the reasons for the disagreement?

We investigated the reason for the disagreement and found that it arose from the image processing. We have improved the image processing algorithm (which mainly involved changing the order in which corrections were applied). We have adjusted the text in Sections 2.2 and 4.2 accordingly:

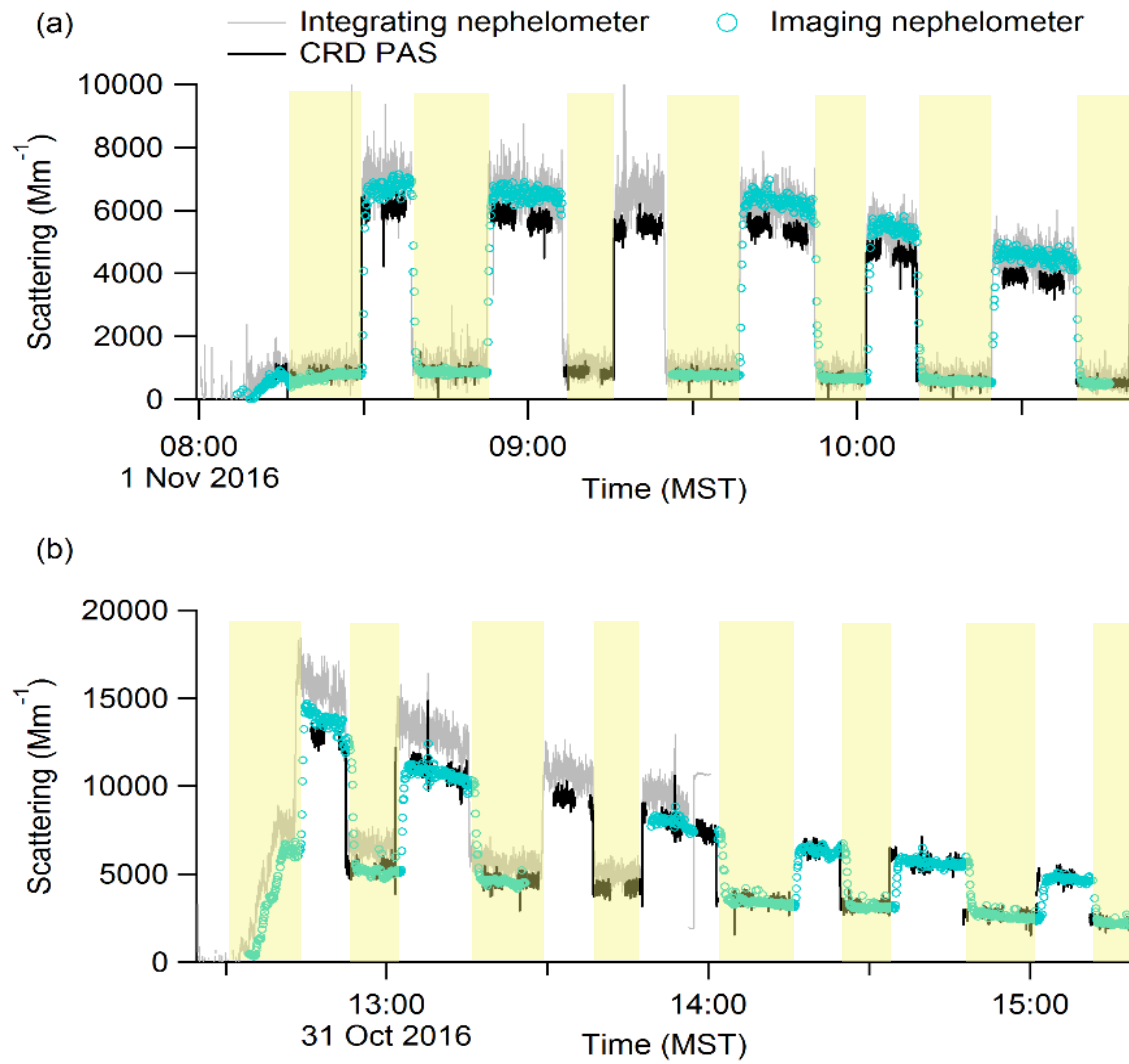
Section 2.2:

P.4 L.1 – P.5 L.3: “The raw CCD images were processed in five steps to produce an aerosol scattering phase function by correcting for the CCD dark background, scattered light due to internal surfaces, and Rayleigh scattering. First, a dark background spectrum was subtracted from each CCD image. This is necessary because CCD detectors produce non-zero dark current in the absence of light due to thermal noise and an electronic offset. The dark background image was acquired with the same integration time as the aerosol images and was measured before each fire. Second, light scattering from surfaces within the sample volume was removed by subtracting a laser power-normalized correction from each image. The scattering correction was determined by filling the chamber with helium, which has a negligible scattering coefficient, and taking an average of ~20 images at each wavelength in order to account for light reaching the CCD from the instrument body and optics. Third, *each strip of the corrected image was integrated and an additional constant offset likely due mainly to temperature variations in the CCD pixel array was removed.* Fourth, *the Rayleigh scatter contribution of the dry air, which was measured before each experiment, was pressure-corrected and removed from the signal to determine the aerosol-only scattering.* ~~additional background scattering was removed by averaging the signal level of the “dark” pixels as shown in Figure 2. This background was attributed to temperature variations in the CCD pixel array.~~ Finally, *each strip of the corrected image was integrated, and an angle-dependent correction factor was applied.* This correction factor was determined daily using Rayleigh scattering from dried and filtered ambient air. The consistency of the calibration factor from day-to-day (<3% variation) implies that the lens, window, and chamber walls did not accumulate particles or become dirty over time. ~~Finally, the Rayleigh scatter contribution of the dry air was calculated based on the instrument pressure and temperature, and removed from the signal to determine the aerosol only scattering.~~“

Section 4.2:

P.9 L.32 – P.10 L.2: “~~The higher value for the integrating nephelometer scattering is likely due to errors arising from extrapolating from 450 nm, however the~~ The good agreement between *all three measurements* the CRD PAS and imaging nephelometer provides confidence in the total scatter retrieved by the imaging nephelometer (see Figure S4 S6 in Supplementary for correlation plot).”

P.10 L.17-19: “~~There is greater disagreement between the three different measurements of total scatter at 405 nm for this fire, although the CRD PAS and imaging nephelometer agreement becomes much better at later times in the experiment. The CRD PAS and imaging nephelometer agree well throughout this experiment. The higher scattering retrieved by the integrating nephelometer is likely due to errors arising from extrapolating from 450 nm.~~”



* Page 10: While discussing figure 4, it would be good to provide some more details (here or earlier on would be fine too) on the details of the RDG calculations.

We have added in references that the reader can look to for more information on the formulae involved in calculating the scattering phase function for the RDG model in Section 3.1:

P.8 L.8-9: “The scattering angle-dependent structure factor, which is needed to calculate the allows calculating a-RDG phase function, was adopted from Sorensen et al. (Liu et al., 2013a; Sorensen et al., 1992; Yang and Köylü, 2005). Details of the phase function calculations based on the RDG model can be found in Liu et al. (2013a) and Kandilian et al. (2015).”

* Page 11, lines 4 and 5: “Given the value of the fractal dimension ($D_f = 1.85$)...” maybe I misunderstood, but I thought the D_f was assumed from other work, not measured somehow in this work, so I am not sure how this conclusion can be reached here.

We apologize for the confusion, and realize that without performing a thorough sensitivity analysis it is a bit over-stretching to make statements about fractal collapse based on the qualitative comparison between the RDG model and measurement. We have removed the following sentence:

P.11 L.4-6: “Given the value of the fractal dimension ($D_f = 1.85$) is close to the minimum diffusion-limited case (~1.75), we assume the agglomeration was (nearly) diffusion limited, and no significant restructuring or collapse of the particles occurred in the chamber.”

* Page 11, line 10: in the paper, cited earlier on in the manuscript, by China et al. 2003, an analysis of the changes of tar balls by the thermal denuder is also discussed.

The China et al. citation has been added (P.11 L.10-11).

* Page 11 at the bottom: a discussion of the effect of thermodenuding on fractal aggregates from different fuels is also provided in a recent paper by Bhandari et al., Effect of Thermodenuding on the Structure of Nascent Flame Soot Aggregates. *Atmosphere*, 2017. 8(9): p. 166.

We are grateful for the very helpful suggestion to look at this paper. We have added the following text:

P. 11 L.30-31: “...(Skillas et al., 1998). Additionally, soot agglomerates emitted by ethylene and methane flames did not exhibit restructuring after being heated to 250 – 270°C (Bhandari et al., 2017). If the fractal particles underwent restructuring..”

- **Figure 2. Caption:** “The laser axis is curved due to the alignment with respect to the wide-angle lens.” Please clarify.

We have tried to clarify this caption as follows:

P.21 L.5: “~~The laser axis is curved due to the alignment with respect to the wide-angle lens. The blue dashed line shows the center of the laser beam; the slight curvature arises from the wide-angle lens being slightly off-center relative to the laser path.~~”

- **Figures 6 and 8 How are the different curves normalized?**

In the literature, phase functions are typically normalized either for the total integral over all solid angles equal to unity or forward scatter (0°) equal to unity. We understand that the former method (which was used in the original manuscript) may be somewhat confusing, and is also more sensitive to noise in the side-scattering region where the signal-to-noise-ratio is relatively small. Therefore, in the updated draft we have selected the second method of normalization (normalizing to 5° scattering angle because we cannot measure at 0°). The new figures (P.25,27), with updated captions, are shown here:

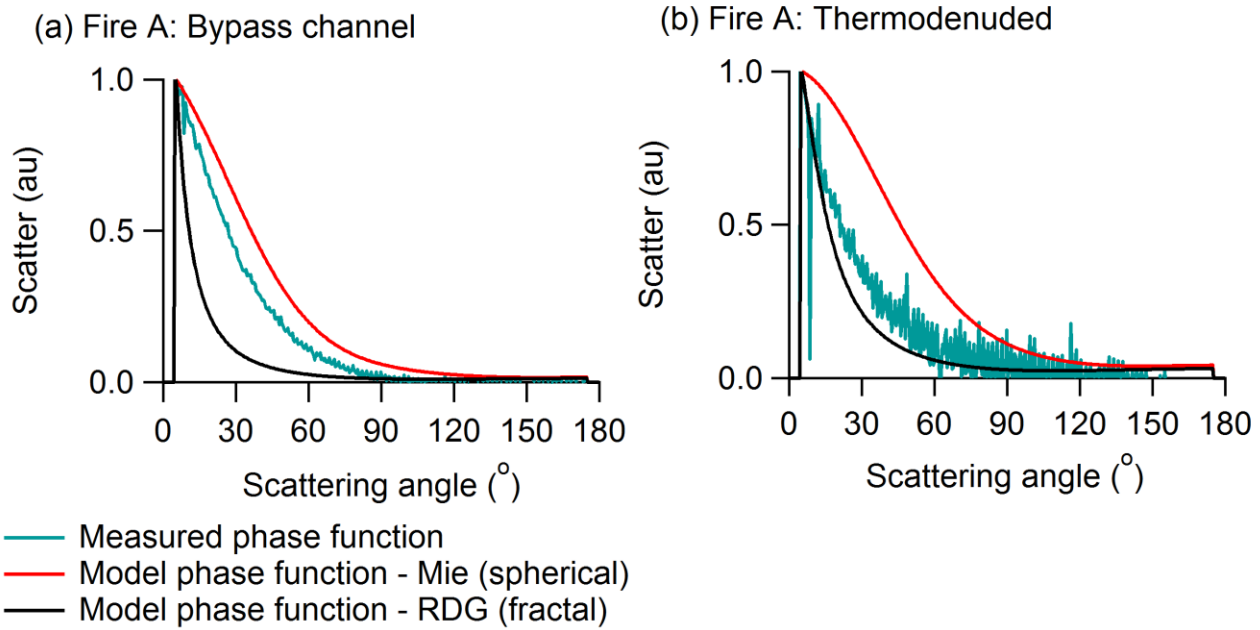


Figure 1: Comparison of measured (blue) phase function at 405 nm to Mie theory model (red) and RDG model (black) for one cycle of sampling through bypass channel (a) and after the thermodenuder (b) for Fire A. Phase functions are normalized to total scatter in spherical coordinates. Phase functions are normalized to unity at 5° scattering angle. Mie theory calculations are based on HULIS refractive index (Dinar et al., 2008) and RDG calculations are based on ponderosa pine parameterization (Chakrabarty et al., 2006).

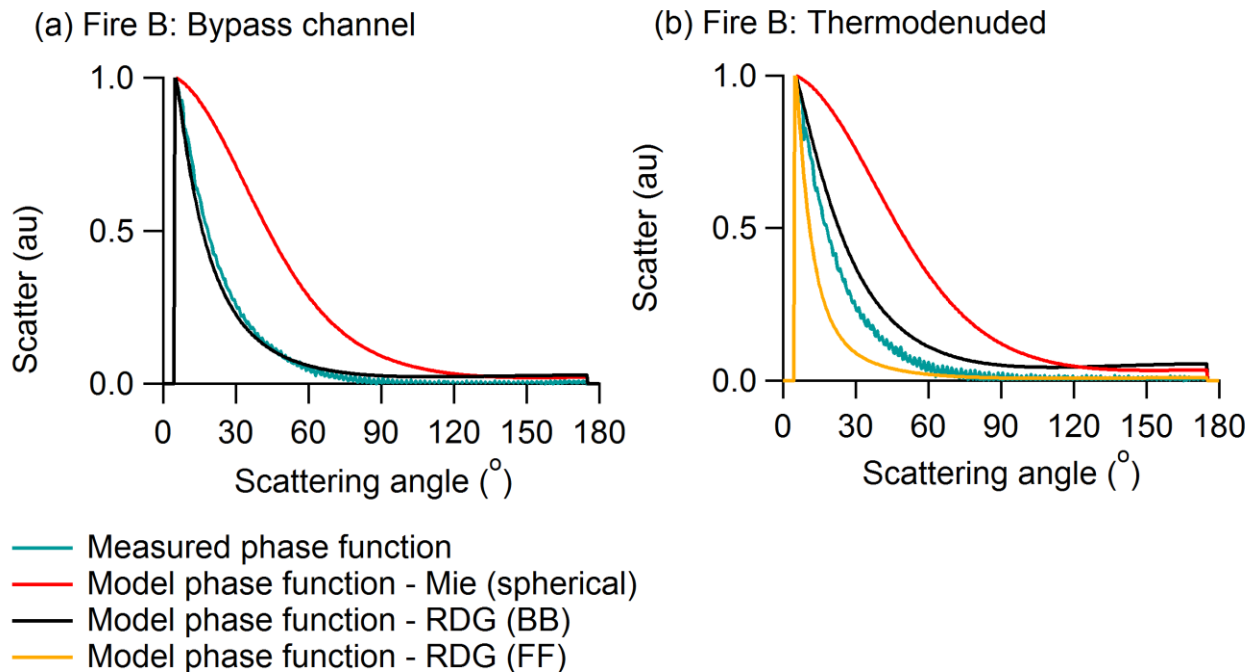


Figure 2: Comparison of measured (blue) phase function at 405 nm to Mie theory model (red) and RDG models (black and orange) for one cycle of sampling through bypass channel (a) and after the thermodenuder (b) for Fire B. Two RDG parameterizations were compared: fossil fuel (FF; orange) and biomass burning (BB; black). Phase functions are normalized to total scatter in spherical coordinates. Phase functions are normalized to unity at 5° scattering angle. Mie theory calculations are based on HULIS refractive index (Dinar et al., 2008) and RDG calculations are based on sage fuel for biomass burning (BB) case (Chakrabarty et al., 2006) and laboratory combustion of fossil fuels (FF) (Sorensen, 2001).